SEMARAK ILMU PUBLISHING

Journal of Advanced Research in Micro and Nano Engineering

Journal homepage:
https://semarakilmu.com.my/journals/index.php/micro_nano_engineering/index
ISSN: 2756-8210

Effect of Silver Doping on the Microstructure and Photocatalytic Performance of Ag-TiO_2 Coatings on Unglazed Ceramic

Norhafizah Zaharuddin[1], Jariah Mohamad Juoi[1,*], Zulkifli Mohd Rosli[1], Nur Dalilah Johari[2], Toshihiro Moriga[3]

[1] Faculty of Industrial and Manufacturing Technology and Engineering, Universiti Teknikal Malaysia Melaka, 76100 Durian Tunggal Melaka, Malaysia
[2] Faculty of Mechanical Engineering, Universiti Teknologi Malaysia, 81310 Johor Bahru, Johor, Malaysia
[3] Department of Applied Chemistry and Engineering, Faculty of Science and Engineering, Tokushima University, Tokushima, 770-8506 Japan

ARTICLE INFO

Article history:
Received 11 August 2024
Received in revised form 17 September 2024
Accepted 20 October 2024
Available online 30 November 2024

Keywords:
Unglazed ceramic tile; Ag-TiO_2 coating; sol gel dip coating; Ag mol %

ABSTRACT

TiO_2 coating photocatalytic activity is limited to short-wavelength ultraviolet (UV) irradiation. To extend its potential to the visible range, doping with semiconductors such as silver (Ag) has been proposed. The optimal amount of Ag incorporation is still under investigation. High Ag concentrations can decrease surface charge, causing agglomeration of Ag species and reduction to Ag° particles on the TiO_2 surface. On the other hand, lower Ag concentrations lead to the formation of AgO, Ag_2O and Ag°. In this study, Ag-TiO_2 coatings were deposited on unglazed ceramic tiles using the dip coating method, with silver contents of 2.5, 5 and 7.5 mol %. The effects of Ag content on the crystalline phase, crystal size, elemental distribution, morphology and cross-sectional surface were analysed. The coatings were heat-treated at 500 °C and characterized using X-ray diffraction (XRD), scanning electron microscopy (SEM) and field emission scanning electron microscopy (FESEM). Photocatalytic performance was evaluated through the degradation of methylene blue under both UV and visible light irradiation. XRD analyses revealed the presence of anatase, rutile, Ag_2O and metallic Ag in all samples. The degree of crystallinity and anatase crystallite size increased with higher Ag content. Surface morphology showed visible cracks and a dense surface at 2.5 and 5 mol % Ag, while the 7.5 mol % Ag coating exhibited a wavy surface. Energy-dispersive X-ray spectroscopy (EDS) on the surface and cross-sectional layers confirmed the presence of Ti, O and metallic Ag particles. The Ag-TiO_2 coating with 2.5 mol % Ag demonstrated better photocatalytic activity under UV light irradiation, while the 7.5 mol % Ag coating exhibited the highest photocatalytic activity under visible light irradiation.

1. Introduction

The development of self-cleaning, bacteria-free surfaces is an important area of research. Meeting the demand for safe, hygienic surfaces presents significant challenges, particularly in

* *Corresponding author.*
E-mail address: jariah@utem.edu.my

https://doi.org/10.37934/armne.25.1.1426

improving existing formulation. Photocatalytic surfaces, which offer antibacterial properties, have been studied using various photocatalysts such as zinc oxide (ZnO), iron (II) trioxide (Fe_2O_3), zirconium dioxide (ZrO_2), magnesium oxide (MgO) and copper (II) oxide (CuO). However, these photocatalysts generally exhibit relatively weak activity compared to titanium dioxide (TiO_2). Consequently, TiO_2 has attracted considerable interest in research and industry due to its favourable properties, including low cost, non-toxicity, photochemical stability, resistance to photo corrosion, photosensitivity, low operational temperature, low energy consumption and ease of synthesis [1-5]. Despite these advantages, TiO_2 faces significant limitations, such as a wide band gap energy (3.2 eV), rapid electron-hole recombination, small surface area and poor conductivity [6-9]. To address these issues, researchers have introduced metal dopants into the TiO_2 lattice, with silver (Ag) being a notable example. Ag can be incorporated as either metal powder or liquid ionic type, successfully broadening the photo response range from the UV to the visible light region. This additional absorption is attributed to the plasmonic properties of Ag [6]. The anatase phase of TiO_2 exhibits lower electron energy than metallic Ag, leading to the formation of a Schottky barrier at the interface between Ag nanoparticles and TiO_2 [9,10].

Various studies have explored the enhancement of TiO_2 properties through metal doping. Khojasteh *et al.,* [11] synthesized Ag-doped SnO_2/TiO_2 photoanodes, achieving a photon-to-electron conversion efficiency of 6.93% in dye-sensitized solar cells—significantly higher than that of TiO_2 photoanodes alone. Onna *et al.,* [12] investigated tungsten-loaded TiO_2 coatings on glazed ceramic tiles, finding them suitable for industrial applications as self-cleaning and antimicrobial surfaces. Ashraf *et al.,* [13] achieved higher photocatalytic performance by evenly distributing nanoparticles between graphene sheets in Ag-doped TiO_2 nanocomposites. Abbad *et al.,* [14] research had demonstrated that adding 10 % Ag dopant to TiO_2 significantly improved photocatalytic activity by lowering the band gap energy from 3.22 eV to 2.67 eV. It can be observed that the amount and form of Ag used in various studies (in terms of its ratio, weight, molarity and percentage) significantly influence the microstructure and photocatalytic performance of TiO_2. Ag dopants can affect the surface coating's texture such as producing smooth, coarse, tearing, or porous surface and can either remain on the surface or diffuse into the TiO_2 matrix. The form of Ag presence either in a form of ion, oxide, or metal also plays a crucial role in enhancing photocatalytic and antimicrobial activity [15,16]. However, excessive Ag can negatively impact these properties by promoting photo hole trapping, which reduces photocatalytic efficiency. Optimal Ag content effectively captures photo induced electrons, facilitating their transfer to oxygen adsorbed on TiO_2 surfaces and increasing the amount of surface hydroxyl radicals [17].

This study focuses on the preparation of Ag-TiO_2 sol using the sol-gel dip coating method, with Ag introduced at 2.5 %, 5 % and 7.5 % mol into TiO_2 sol and deposited on unglazed ceramic tile surfaces. The objective is to examine the presence of Ag on the coated tiles, its influence on crystalline phase formation and microstructure and how these properties relate to photocatalytic performance.

2. Methodology

2.1 Preparation of Ag-TiO_2 Sol and Deposition

Ag-TiO_2 sol was prepared by adding titanium (IV) isopropoxide to 64 ml of deionized water (DI) under constant stirring. While stirring, 0.4 ml of hydrochloric acid was added drop by drop over a period of approximately 3 hours using a pipette. Subsequently, $AgNO_3$ precursors at concentrations of 2.5 mol %, 5 mol % and 7.5 mol % were carefully dissolved in acetonitrile, serving as a reducing agent, before being added to the sol to form the Ag-TiO_2 sol. This sol was stirred for 1 hour and then left to age at room temperature for 48 hours. Unglazed tiles, cut to dimensions of 20 mm x 10 mm x

4 mm, were first cleaned to remove any contaminants by immersion in acetone, ethanol and distilled water for 10 minutes each in an ultrasonic bath. The cleaned tiles were then oven-dried at 110°C for 2 hours before undergoing the dip-coating procedure using a mechanical dip coater (TEFINI Model DP1000) set at a speed of 30 mm/min and a dwelling time of 5 seconds. The coated tiles were allowed to dry for 3 hours and then oven-dried at 110°C for 30 minutes before the next coating layer was applied. This dipping process was repeated 5 times to achieve a homogeneous and high-quality coating layer. Finally, the Ag-TiO_2 coatings deposited on the unglazed tiles were heat-treated at 500°C with a heating rate of 2°C/min.

2.2 Characterization

The crystallinity of the coated tiles was analysed using X-ray diffraction (XRD) with a PANalytical X'PERT PRO MPD Model PW 3060/60, utilizing Cu Kα radiation (λ = 1.54060 Å). The XRD was operated at 40 kV and 30 mA, with a diffraction angle (2θ) ranging from 10° to 80° and a grazing angle of 4°. The collected data were analysed using X'Pert High Score pattern processing software. The average crystallite size (D) was calculated by applying the Scherrer equation to the anatase (A) and rutile (R) peaks at the highest intensity, appearing at 2θ = 25° (101) and 27° (110):XRD PANalytical X'PERT PRO MPD Model PW 3060/60 with Cu Kα radiation (λ = 1.54060 Å) operating at 40 kV and 30 Ma with diffraction angle at 2θ range between 10°- 80° and glazing angle of 4° was used to identify the crystallinity of coating tiles. Data collected and analyse by X'Pert High Score pattern processing. The average crystallite size D was calculated by applying Scherer equation to the anatase (A) and rutile (R) peak at highest intensity peak appears of 2θ = 25° (101) and 27° (110) using Eq. (1).

$$D = \frac{k\lambda}{\beta \cos \theta} \tag{1}$$

Where, k is a constant (k = 0.94), λ is the X-ray wavelength (0.15406 nm), β is the full width at half maximum of the diffraction peak (in radians) and θ is the Bragg angle.

The surface of the Ag-TiO_2 coating on unglazed ceramic tiles was examined using a Scanning Electron Microscope (SEM), JEOL model JSM-6010PLUS/LV and a Field Emission Scanning Electron Microscope (FESEM) coupled with Energy Dispersive X-ray Spectroscopy (EDX), model HITACHI SU5000.

2.3 Photocatalytic

Photocatalytic was measured by degradation of methylene blue performed following the ISO 10678:2010. Two different power sources of 40 watts (UV) and 200 watts (Visible) irradiation were used. Coated tiles need to undergo photocatalytic oxidation process by exposed under UV light for 24 h to decompose or removing any possible organic contaminants known as photocatalytic oxidation process. After that, the samples were left in the dark for 24 h in 25 ml aqueous MB solution known as conditioning solution. This is to ensure the ability of the substrate to absorb dye molecules. Solution containing samples was replaced with the new 25 ml test solution and exposed to the UV and Visible light irradiation for 5 hours. The degradation of MB solution for each sample were measured at 1 h interval and 5 h and determined using UV-Vis spectrometer at adsorption spectrum of 664 nm wavelength. The reference sample (control) was left in the dark and the absorption spectrum also measured at the same time interval. The specific degradation rate, R was calculated as follows:

The photocatalytic activity was measured by the degradation of methylene blue (MB) according to ISO 10678:2010. Two different power sources, 40 watts (UV) and 200 watts (Visible) irradiation, were used. The coated tiles were first exposed to UV light for 24 hours to decompose any possible organic contaminants in a process known as photocatalytic oxidation. After this, the samples were immersed in 25 ml of an aqueous MB solution and kept in the dark for 24 hours, a step referred to as conditioning. This step ensures the substrate's ability to absorb dye molecules.

Following conditioning, the solution containing the samples was replaced with a fresh 25 ml test solution and the samples were exposed to UV and Visible light irradiation for 5 hours. The degradation of the MB solution for each sample was measured at 1-hour intervals over the 5-hour period using a UV-Vis spectrometer at an absorption wavelength of 664 nm. A reference sample (control) was kept in the dark and its absorption spectrum was measured at the same time intervals.

The specific degradation rate, R, was calculated as in Eq. (2).

$$\mathrm{R} = \frac{\Delta A_{\lambda} \times \mathrm{V}}{\Delta \mathrm{t} \times \varepsilon \times \mathrm{d} \times \mathrm{A}} \tag{2}$$

Where ΔA_{λ} is the absorption difference from one measurement to another (1 h to 5 h); V is the volume of MB solution used; Δt is the time difference; ε is the molar extinction coefficient of MB at 664 nm (ε = 7402.8 m^2/mol); d is the measuring cell length used at the spectrophotometer; and A is the contact area of MB solution and the catalyst.

The degradation rate, R of the irradiated and dark samples is then use to calculate the specific photocatalytic activity, P_{MB} using Eq. (3).

$$P_{MB} = R_{irr} - R_{dark} \tag{3}$$

Finally, the photonic efficiency, $\zeta_{MB}$of the samples is calculated using Eq. (4).

$$\zeta_{MB} = P_{MB} / E_P \times 100 \tag{4}$$

Where E_P is the light radiation intensity (W/m^2).

3. Results

3.1 Phase Transformation

Figure 1 shows the X-ray diffraction patterns of undoped and Ag-doped TiO_2 on unglazed tiles. The TiO_2 coating primarily consists of the rutile phase (JCPDS: 00-021-1276) with prominent peaks at 2θ = 26.4° (111), 27.9° (210) and 68.03° (213). The brookite phase (JCPDS: 00-029-1360) is identified at 2θ = 36.4° (232) and 41.3° (002), while a single peak of the anatase phase (JCPDS: 00-021-1272) appears at 2θ = 59.91° (208). Incorporating 2.5, 5 and 7.5 mol % Ag into the TiO_2 coating induces the growth of metallic Ag (JCPDS: 00-041-1402) and Ag oxide (JCPDS: 00-041-1104) peaks. The Ag phase is detectable even at the lowest Ag content of 2.5 mol%, with more pronounced Ag peaks as the Ag content increases to 7.5 mol%.

The TiO_2 phases of anatase, rutile and brookite remained present at the same angles, although some peaks were overtaken by Ag peaks. Metallic Ag-4H, indicating a hexagonal structure, appeared at 2θ = 32.29° (104), 50.59° (203) and 59.88° (001). Ag_2O was present at 2θ = 54.9° (331). As the Ag content increased, the growth of metallic Ag was inhibited and the Ag_2O peak became sharper, indicating a gradual increase in Ag oxide intensity. This Ag_2O peak will eventually disappear and the absence of oxidized forms in the XRD pattern suggests the presence of Ag in a metallic state, as

proposed by Gong [18]. The presence of AgO and Ag_2O phases with increasing Ag content was also revealed by Noberi [19], who worked on Ag-TiO_2 nanostructures on Ni filters with 10 wt% and 15 wt % Ag content.

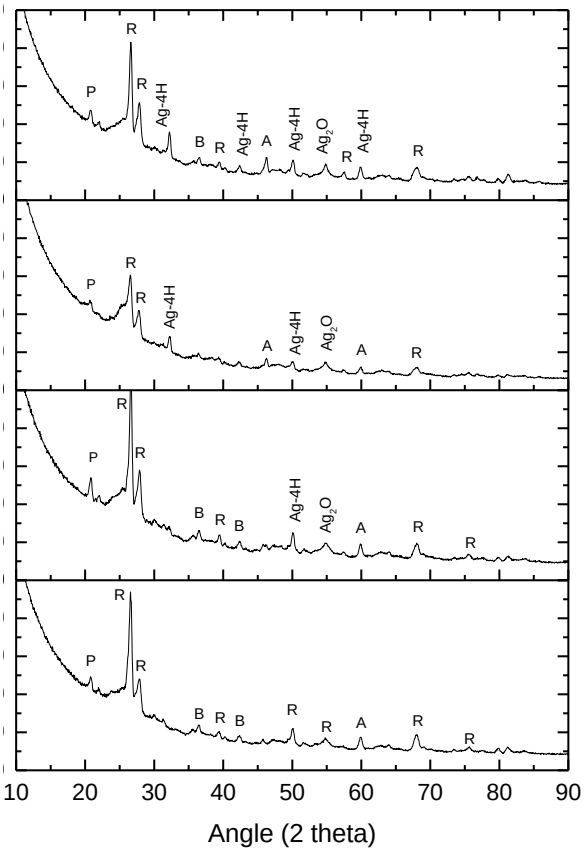

Fig. 1. XRD pattern of Ag-TiO_2 coating deposited on unglazed tile

The anatase crystallite sizes of the undoped and Ag-doped TiO_2 coatings on unglazed tiles at different Ag contents are shown in Table 1. The anatase crystallite size of the undoped TiO_2 coating was 8.6 nm. With Ag incorporation, the anatase crystallite size increased as the Ag content increased. This observation aligns with the findings of Saraswati *et al.,* [20], who reported that the crystal size of anatase TiO_2 (P25) was 20 nm, while Ag/TiO_2 was 39 nm. Generally, Ag acts as an electron trap, occupying positions in the matrix and preventing electron-hole recombination rather than forming a separate crystal. However, Vakhrushev *et al.,* [21] also noted that the average crystallite size of anatase, rutile and silver-modified titanium (IV) oxide increased with Ag concentration up to 5.0 x 10^{-2} mol/L, with no further effect on crystallite size beyond this concentration. On the contrary, research by Aini *et al.,* [22] on silver-doped TiO_2 photocatalysts synthesized by the sonochemical method reported smaller anatase crystallite sizes for doped TiO_2 compared to undoped TiO_2. Thus, crystallite sizes can also be influenced by the synthesis method used. The increase in anatase crystallite size of Ag-TiO_2 doped on unglazed tiles indicates better crystallinity of the coating, suggesting that coating defects and dislocations decrease with increased Ag content [2]. The XRD data analysis shows that increasing the silver content from 2.5 to 7.5 mol% led to an increase in the degree of crystallinity. This is likely due to the phase transformation of TiO_2 accompanying the decomposition of silver nitrate [21]. The increased crystallite size indicates that the strain in the Ag-TiO_2 coating increases to stabilize the crystal structure [23]. This means the crystallite size increases initially to release the strain and stabilize the crystal structure.

Table 1
Anatase crystallite size of TiO_2 and Ag-TiO_2 coating deposited on unglazed tile

Photocatalyst sample	Crystallite size
TiO_2	8.6
2.5 mol % Ag-TiO_2	24.3
5 mol % Ag-TiO_2	26.2
7.5 mol % Ag-TiO_2	36.6

The Full Width at Half Maximum (FWHM) is influenced by strain, grain size and crystal imperfections. The FWHM for the (101) diffraction plane at angles $23° < \theta < 27°$ from the XRD data of Ag-TiO_2 coatings on unglazed tiles was calculated and is presented in Figure 2. The FWHM values for TiO_2 and Ag-TiO_2 coatings on unglazed tiles were computed as 0.344, 0.295, 0.590 and 0.393, respectively. The FWHM increased with Ag content up to 5 mol % and decreased when the Ag content reached 7.5 mol %. Li *et al.,* [23] studied the effect of Cu doping at different concentrations on PbS nanofilms, noting that the FWHM of Cu-doped PbS films initially decreased and then increased. This behaviour was explained by the preferential incorporation of Cu ions into defect sites within the crystal, which reduced the system's free energy. This reduction in microstrain and dislocation density promoted the crystallization process. Similarly, when Ag was introduced into TiO_2, the FWHM decreased at 2.5 mol % Ag, increased at 5 mol % Ag and decreased again at 7.5 mol % Ag. This pattern is consistent with Li *et al.,* findings [23]. It can be deduced that Ag ions tend to occupy defect sites in the TiO_2 crystal, promoting crystallization. The observed fluctuations in FWHM indicate efforts to stabilize the crystal structure.

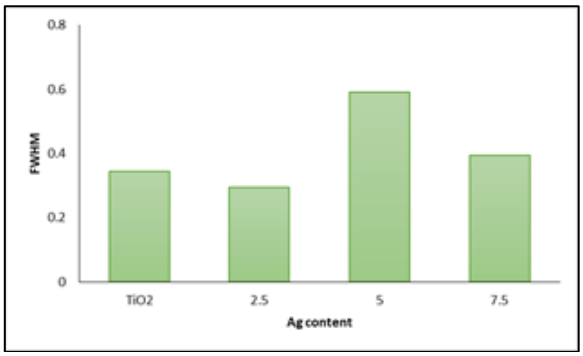

Fig. 2. FWHM of Ag-TiO_2 coated on unglazed tile

3.2 Surface Morphology and Elemental Mapping

Table 2 shows the surface morphology and EDX mapping of the Ag-TiO_2 coating deposited on unglazed tiles. The TiO_2 coating without Ag incorporation exhibits numerous visible mud-crack patterns across the entire surface. This observation is consistent with findings by Musa *et al.,* [24] and Demircia *et al.,* [2], who reported that such cracks occur due to restructuring and relaxation during the heat treatment process. The thermal shock associated with the heat treatment regime of TiO_2 coatings can lead to non-uniform and cracked surfaces, reducing the coating's lucidity and transparency [25]. When Ag was incorporated into the TiO_2 coating, the surface morphology of the 2.5 mol % Ag-TiO_2 coating did not differ significantly from the pure TiO_2 coating. The density of the cracks remained unchanged, indicating that the small amount of Ag did not improve the surface coating. As the Ag content increased to 5 mol %, smaller, uneven cracks appeared across the surface. At 7.5 mol % Ag, the coating showed fewer cracks and a wavy appearance. However, visible pores on

the surface suggested coating peel-off. The increased Ag content also led to the appearance of small particles spread across the surface, identified as Ag particles by SEM/EDX mapping. During the crystallization process, Ag^+ ions migrated to the TiO_2 surface, contributing to the formation of Ag and/or Ag^2O [26]. The coating surfaces were well-covered and uniformly distributed with Ti, O and Ag particles. The EDX spectra revealed clear peaks at 0.5 keV, 4.5 keV and 4.9 keV for titanium and a peak around 0.5 keV for oxygen. The peaks for Ag appeared at 3 keV and 2.7 keV with low intensity. These peak signals were similar to those reported by Tijani *et al*., [27]. The strong peak at 2 keV for Au was due to the sputter coating during sample preparation.

Ling *et al.,* [4] also reported the uniform distribution of Ag on the TiO_2 surface in their investigation of the photocatalytic properties of Ag/TiO_2. The Ag, Ti and O particles were closely associated, facilitating phase transformation [21]. Ag atoms coordinated with oxygen atoms on the anatase crystallites, confirming the presence of Ag_2O detected by XRD. The distribution of Ag overlapped with Ti and O spots, suggesting that Ag could exist as AgO, Ag_2O, or metallic Ag, as identified in XRD results. Ag^+ ions tended to migrate from the TiO_2 grains to their surfaces and ultimately to the TiO_2 film surface. The larger size of Ag^+ ions (approximately 126 pm) compared to Ti^{4+} ions (approximately 68 pm) restricted their diffusion into the anatase lattice phase [28,29]. At 7.5 mol% Ag, the uneven coating and agglomeration of particles resulted in a wavy, coarse surface, leading to instability and a decrease in the number of TiO_2 nanoparticle nuclei. This is supported by Mahdieh [30], who found that increasing $AgNO_3$ concentration from 0.005 % to 0.1 % (w/v) decreased the number of nuclei due to instability and agglomeration.

Table 2
SEM and elemental mapping of Ti, Oxygen and Ag for Ag-TiO_2 coating deposited on unglazed tile

Surface morphology	EDX spectrum
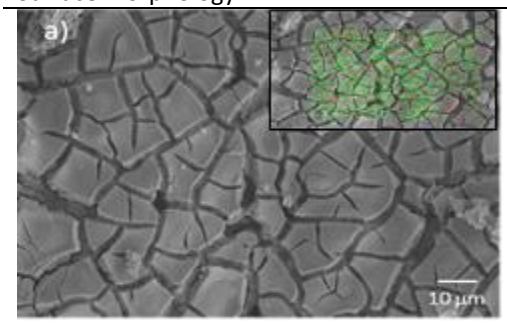	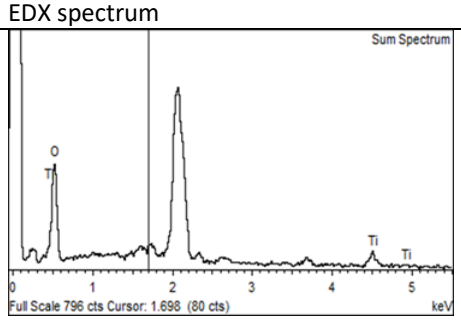
TiO_2	
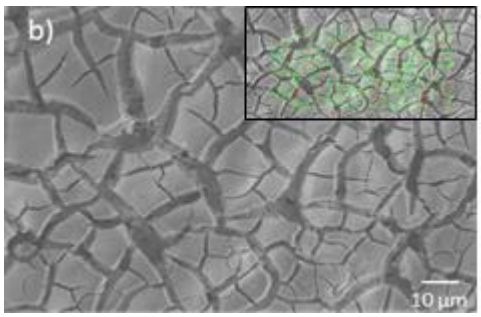	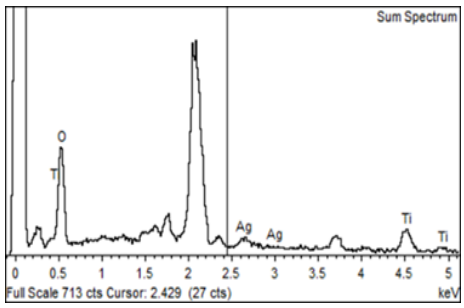
2.5 mol % Ag	

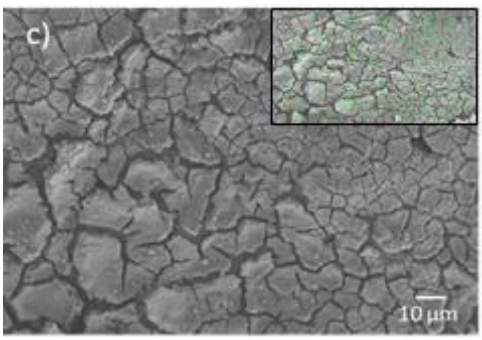

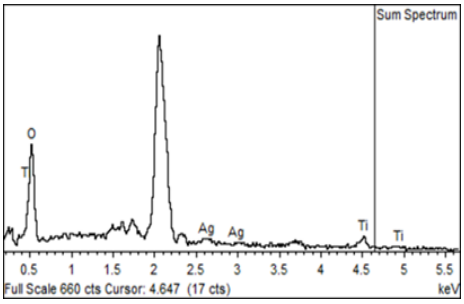

5 mol % Ag

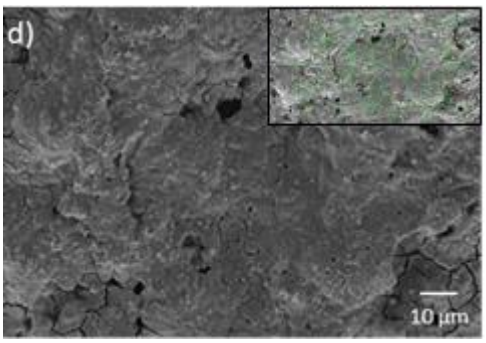

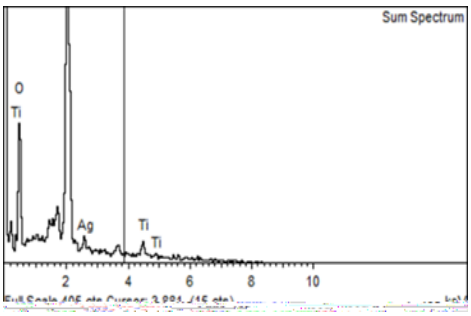

7.5 mol % Ag

3.3 Surface Cross Section

The Ag-TiO_2 coating on unglazed tiles shows that the coating layer and the substrate cannot be distinguished (Table 3). Due to the nature of unglazed ceramic tiles, the rough surface, with a measured roughness of 4.46 ± 0.02 µm and the porous structure tend to absorb the Ag-TiO_2 coating sol rather than forming a distinct layer. Liquids filling the pores of unglazed ceramic tiles cover the surfaces and, in this case, the Ag-TiO_2 coating has filled the pores and been absorbed by the tile surface, making it difficult to differentiate between the coating layer and the substrate. Therefore, the thickness of the Ag-TiO_2 coating layer on the unglazed tiles could not be determined. This finding is consistent with Musa *et al.,* [24], who noted that the cross-section of TiO_2 coating on unglazed tiles without the addition of Degussa P25 is indistinguishable from the substrate, making thickness determination impossible. During the dip coating process, the Ag-TiO_2 sol diffused into the unglazed ceramic tiles, resulting in the presence of Ti, O and Ag elements within the layer. The high porosity of unglazed ceramic tiles (34 %) facilitated the diffusion of the sol into the substrate. Elements such as silicon (Si), calcium (Ca), aluminium (Al) and sodium (Na) were also detected, as they are components of the unglazed ceramic tile substrate. Other elements, such as gold (Au), palladium (Pd) and carbon (C), likely originated from the sample preparation for SEM/EDX testing.

Table 3
Cross section of Ag-TiO_2 coating deposited on unglazed tile

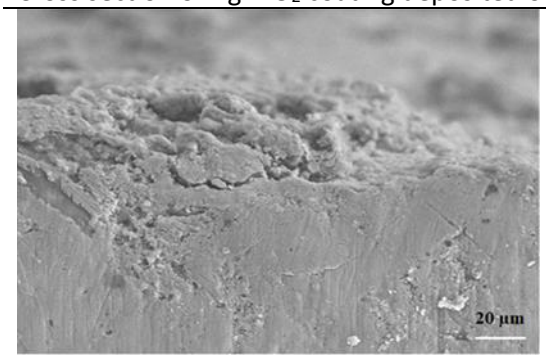	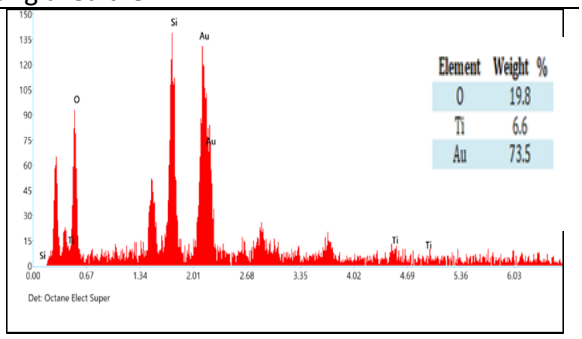	TiO_2
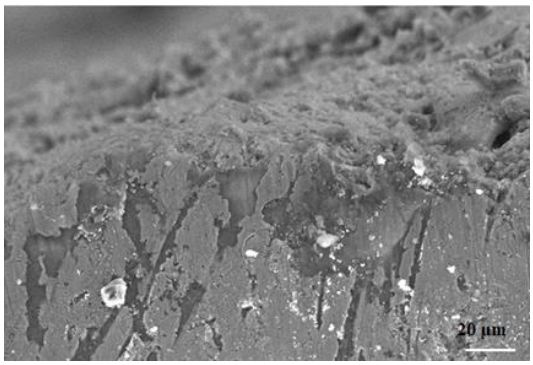	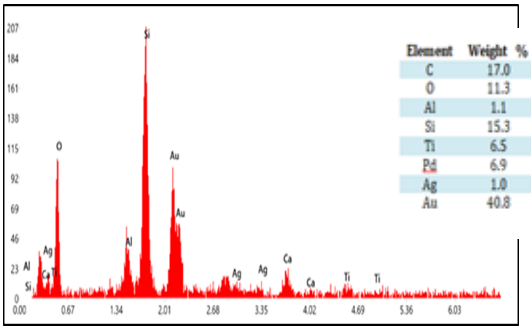	2.5 mol % Ag
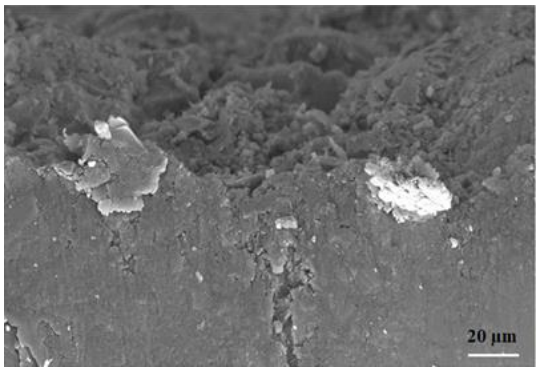	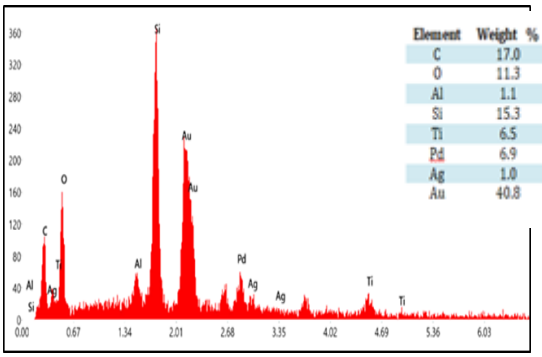	5 mol % Ag
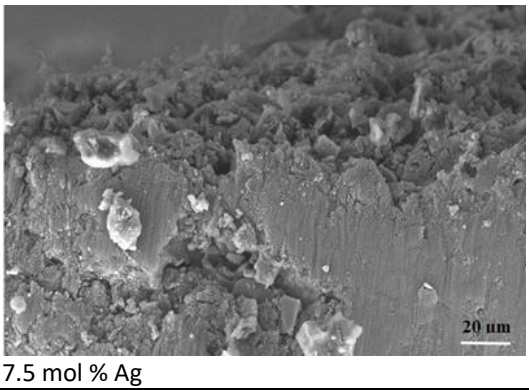	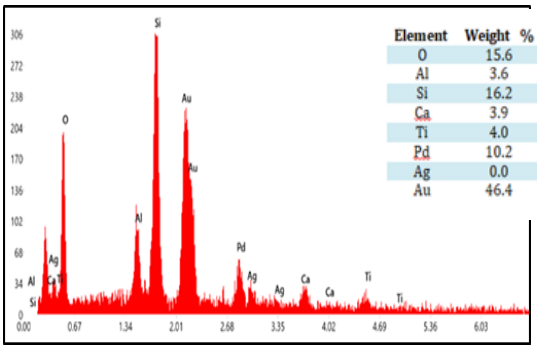	7.5 mol % Ag

3.4 Photocatalytic Performances

Table 4 presents the photocatalytic activity of Ag-TiO_2 coatings on unglazed tiles under UV and visible light irradiation. The results indicate that the photocatalytic activity of the Ag-TiO_2 coated tiles under UV light does not significantly change with increasing Ag content. The highest photocatalytic activity under UV light was observed at 2.5 mol % Ag. In contrast, under visible light, the photocatalytic activity peaked at 5 mol % Ag, which can be attributed to the fewer cracks and presence of pores in the coating layer, as observed in SEM images. The pores enhance the photocatalytic activity of the coating surfaces. This finding aligns with the study by Ying *et al.,* [31], which reported that Ag doping in TiO_2 does not enhance photocatalytic activity under UV light but significantly increases it under visible light due to effective electron-hole separation. For UV light exposure, the highest photocatalytic activity at 2.5 mol % Ag can be explained by the effectiveness of a small amount of Ag in degrading pollutants at wavelengths ≤340 nm. Additionally, the balanced presence of Ag_2O and metallic Ag at this concentration actively reacts under UV light. Since Ti is generally active under UV irradiation and the amount of Ti decreases with increasing Ag content, the higher Ti content at 2.5 mol % Ag contributes to higher photocatalytic activity.

Furthermore, EDX cross-section analysis showed that the Ti content was highest at 2.5 mol % Ag, supporting the observed high photocatalytic activity under UV light. The Ag ions in the 2.5 mol % Ag-TiO_2 layer assist in degrading methylene blue effectively due to UV light penetration of the substrate surface. Under visible light irradiation, the 5 mol% Ag -TiO_2 coating exhibited the highest photocatalytic activity compared to 2.5 mol % and 7.5 mol % Ag coatings. EDX cross-section analysis revealed that the Ag ions were approximately 1 wt % at 5 mol % Ag, suggesting that most Ag ions had diffused to the coating surface and were actively responding to visible light, which does not penetrate the substrate. The high photocatalytic activity at 5 mol % Ag is also attributed to the optimal anatase crystallite size, which compensates for reduced performance due to coating defects and dislocations. Therefore, the photocatalytic activity of Ag-TiO_2 coatings on unglazed tiles varies with Ag content and light irradiation type, demonstrating different responses under UV and visible light exposure. It should be also noted that the photocatalytic activity is also influenced the time of exposure and dye concentration during the photocatalytic test [32].

Table 4
Photocatalytic activity of Ag-TiO_2 coating deposited on unglazed tile exposed under UV and Visible light

Samples	UV light, P_{mb} (mol/m^2h)	Visible light P_{mb} (mol/m^2h)
TiO_2	4.53×10^{-5}	5.05×10^{-6}
2.5 mol % Ag-TiO_2	$5.5.6 \times 10^{-6}$	4.49×10^{-7}
5 mol % Ag-TiO_2	4.73×10^{-6}	8.06×10^{-6}
7.5 mol % Ag-TiO_2	4.78×10^{-6}	5.44×10^{-6}

4. Conclusions

In conclusion, this study investigated the fabrication and characterization of Ag-TiO_2 coatings on unglazed ceramic tiles, focusing on varying Ag content and its implications on crystallinity, surface morphology, elemental distribution and photocatalytic activity. The sol-gel method was employed to deposit coatings comprising anatase, rutile and Ag phases (Ag_2O and metallic Ag). Increasing Ag content from 2.5 to 7.5 mol % enhanced the crystallinity of the coatings, albeit accompanied by surface defects such as mud cracks and a wavy appearance at higher Ag concentrations. Surface analysis using SEM/EDX revealed the random dispersion of Ti, O and Ag particles, with Ag particles

overlapping Ti and O spots. The rough and porous nature of unglazed ceramic tiles posed challenges in accurately determining coating thickness, complicating differentiation between the Ag-TiO_2 layer and the substrate. Cross-section analysis confirmed diffusion of the Ag-TiO_2 coating into the ceramic tile. Photocatalytic testing under UV and visible light demonstrated distinct responses based on Ag content. The coating with 2.5 mol % Ag exhibited superior photocatalytic activity under UV light, while the 5 mol % Ag coating showed enhanced performance under visible light. These findings highlight the potential of Ag-TiO_2 coatings for mitigating microbial contamination on high-risk surfaces in healthcare settings. Further investigations into their photocatalytic performance under various lighting conditions are recommended to optimize their application indoors and outdoors, particularly in environments requiring stringent cleanliness standards like hospitals. Implementation of such coatings could effectively contribute to minimizing the risk of bacterial infections through tailored surface modifications.

Acknowledgement
This research was funded by a grant from Ministry of Higher Education of Malaysia (FRGS/1/2014/TK04/FKP/02/F00215).

References

[1] Mao, Hui, Zhengxin Fei, Chaoqun Bian, Leilei Yu, Shengyi Chen and Yongteng Qian. "Facile synthesis of high-performance photocatalysts based on Ag/TiO2 composites." *Ceramics International* 45, no. 9 (2019): 12586-12589. https://doi.org/10.1016/j.ceramint.2019.03.109

[2] Demirci, Selim, Tuncay Dikici, Metin Yurddaskal, Serdar Gultekin, Mustafa Toparli and Erdal Celik. "Synthesis and characterization of Ag doped TiO2 heterojunction films and their photocatalytic performances." *Applied Surface Science* 390 (2016): 591-601. https://doi.org/10.1016/j.apsusc.2016.08.145

[3] Hoang, Nhung Thi–Tuyet, Nguyen Van Suc and The–Vinh Nguyen. "Bactericidal activities and synergistic effects of Ag–TiO2 and Ag–TiO2–SiO2 nanomaterials under UV–C and dark conditions." *International Journal of Nanotechnology* 12, no. 5-7 (2015): 367-379. https://doi.org/10.1504/IJNT.2015.067894

[4] Ling, Lili, Yawei Feng, Hao Li, Yao Chen, Jieya Wen, Jian Zhu and Zhenfeng Bian. "Microwave induced surface enhanced pollutant adsorption and photocatalytic degradation on Ag/TiO2." *Applied Surface Science* 483 (2019): 772-778. https://doi.org/10.1016/j.apsusc.2019.04.039

[5] Karagoz, Sultan, N. Burak Kiremitler, Menekse Sakir, Samaa Salem, M. Serdar Onses, Ertugrul Sahmetlioglu, Ahmet Ceylan and Erkan Yilmaz. "Synthesis of Ag and TiO2 modified polycaprolactone electrospun nanofibers (PCL/TiO2-Ag NFs) as a multifunctional material for SERS, photocatalysis and antibacterial applications." *Ecotoxicology and Environmental Safety* 188 (2020): 109856. https://doi.org/10.1016/j.ecoenv.2019.109856

[6] Zheng, Xinlu, Dequan Zhang, Yan Gao, Yongchuan Wu, Qingyun Liu and Xixi Zhu. "Synthesis and characterization of cubic Ag/TiO2 nanocomposites for the photocatalytic degradation of methyl orange in aqueous solutions." *Inorganic Chemistry Communications* 110 (2019): 107589. https://doi.org/10.1016/j.inoche.2019.107589

[7] Qaid, Saif MH, Mukhtar Hussain, Mahmoud Hezam, MA Majeed Khan, Hamad Albrithen, Hamid M. Ghaithan and Abdullah S. Aldwayyan. "Structural and optical investigation of brookite TiO2 thin films grown by atomic layer deposition on Si (111) substrates." *Materials Chemistry and Physics* 225 (2019): 55-59. https://doi.org/10.1016/j.matchemphys.2018.12.067

[8] Zielińska-Jurek, Anna, Zhishun Wei, Izabela Wysocka, Piotr Szweda and Ewa Kowalska. "The effect of nanoparticles size on photocatalytic and antimicrobial properties of Ag-Pt/TiO2 photocatalysts." *Applied Surface Science* 353 (2015): 317-325. https://doi.org/10.1016/j.apsusc.2015.06.065

[9] Thamer, Nidal Hassoun and Oraas Adnan Hatem. "Synthesis and Characterization of TiO2–Ag-Cellulose Nanocomposite and evaluation of photo catalytic degradation efficiency for Congo Red." In *IOP Conference Series: Earth and Environmental Science*, vol. 1029, no. 1, p. 012026. IOP Publishing, 2022. https://doi.org/10.1088/1755-1315/1029/1/012026

[10] Li, Haijin, Yong Zhou, Wenguang Tu, Jinhua Ye and Zhigang Zou. "State-of-the-art progress in diverse heterostructured photocatalysts toward promoting photocatalytic performance." *Advanced Functional Materials* 25, no. 7 (2015): 998-1013. https://doi.org/10.1002/adfm.201401636

[11] Khojasteh, Farzaneh, Mansour Rezaee Mersagh and Hassan Hashemipour. "The influences of Ni, Ag-doped TiO2 and SnO2, Ag-doped SnO2/TiO2 nanocomposites on recombination reduction in dye synthesized solar cells." *Journal of Alloys and Compounds* 890 (2022): 161709. https://doi.org/10.1016/j.jallcom.2021.161709

[12] Onna, Diego, Keyla M. Fuentes, Cecilia Spedalieri, Mercedes Perullini, María Claudia Marchi, Fernando Alvarez, Roberto J. Candal and Sara A. Bilmes. "Wettability, photoactivity and antimicrobial activity of glazed ceramic tiles coated with titania films containing tungsten." *ACS omega* 3, no. 12 (2018): 17629-17636. https://doi.org/10.1021/acsomega.8b03339

[13] Ashraf, Muhammad Aqeel, Zhenling Liu, Wan-Xi Peng, Kittisak Jermsittiparsert, Ghader Hosseinzadeh and Raza Hosseinzadeh. "Combination of sonochemical and freeze-drying methods for synthesis of graphene/Ag-doped TiO2 nanocomposite: A strategy to boost the photocatalytic performance via well distribution of nanoparticles between graphene sheets." *Ceramics International* 46, no. 6 (2020): 7446-7452. https://doi.org/10.1016/j.ceramint.2019.11.241

[14] Abbad, S., K. Guergouri, S. Gazaout, S. Djebabra, A. Zertal, R. Barille and M. Zaabat. "Effect of silver doping on the photocatalytic activity of TiO2 nanopowders synthesized by the sol-gel route." *Journal of Environmental Chemical Engineering* 8, no. 3 (2020): 103718. https://doi.org/10.1016/j.jece.2020.103718

[15] Cherif, Yassine, Hajer Azzi, Kishore Sridharan, Seulgi Ji, Heechae Choi, Michael G. Allan, Sihem Benaissa *et al.,* "Facile synthesis of gram-scale mesoporous Ag/TiO2 photocatalysts for pharmaceutical water pollutant removal and green hydrogen generation." *ACS omega* 8, no. 1 (2022): 1249-1261. https://doi.org/10.1021/acsomega.2c06657

[16] Nyankson, Emmanuel, Dominic Awuzah, Elvis K. Tiburu, Johnson K. Efavi, Benjamin Agyei-Tuffour and Lily Paemka. "Curcumin loaded Ag–TiO 2-halloysite nanotubes platform for combined chemo-photodynamic therapy treatment of cancer cells." *RSC advances* 12, no. 51 (2022): 33108-33123. https://doi.org/10.1039/D2RA05777H

[17] Sobana, N., M. Muruganadham and M. J. J. O. M. Swaminathan. "Nano-Ag particles doped TiO2 for efficient photodegradation of direct azo dyes." *Journal of Molecular Catalysis A: Chemical* 258, no. 1-2 (2006): 124-132. https://doi.org/10.1016/j.molcata.2006.05.013

[18] Gong, Dangguo, Weng Chye Jeffrey Ho, Yuxin Tang, Qiuling Tay, Yuekun Lai, James George Highfield and Zhong Chen. "Silver decorated titanate/titania nanostructures for efficient solar driven photocatalysis." *Journal of Solid State Chemistry* 189 (2012): 117-122. https://doi.org/10.1016/j.jssc.2011.11.036

[19] Noberi, Cansu, Figen Kaya and Cengiz Kaya. "Synthesis, structure and characterization of hydrothermally synthesized Ag-TiO2 nano-structures onto Ni filters using electrophoretic deposition." *Ceramics International* 42, no. 15 (2016): 17202-17209. https://doi.org/10.1016/j.ceramint.2016.08.012

[20] Saraswati, Mustika, Resi Levi Permadani and A. Slamet. "The innovation of antimicrobial and self-cleaning using Ag/TiO2 nanocomposite coated on cotton fabric for footwear application." In *IOP Conference Series: Materials Science and Engineering*, vol. 509, no. 1, p. 012091. IOP Publishing, 2019. https://doi.org/10.1088/1757-899X/509/1/012091

[21] Vakhrushev, A. Yu, T. B. Boitsova, V. V. Gorbunova and V. M. Stozharov. "Effect of silver additions on the structural properties and phase composition of TiO2/Ag composites." *Inorganic Materials* 53, no. 2 (2017): 171-175. https://doi.org/10.1134/S0020168517020157

[22] Aini, Nur, Saoki Rachman, Anik Maunatin and Aminatus Syarifah. "Synthesis, characterization and antibacterial activity of silver doped TiO2 photocatalyst." In *AIP Conference Proceedings*, vol. 2120, no. 1. AIP Publishing, 2019. https://doi.org/10.1063/1.5115693

[23] Li, Rui, Wei Li, Mengting Liu, Qinyu He, Yinzhen Wang, Qiuqiang Zhan and Teng Wang. "Structural, morphological, optical and electrical properties of Cu-doped PbS nanofilms." *ES Materials & Manufacturing* 4, no. 3 (2019): 38-44.

[24] Musa, Muharniza Azinita, Jariah Mohd Juoi, Zulkifli Mohd Rosli and Nur Dalilah Johari. "Effect of Degussa P25 on the morphology, thickness and crystallinity of sol-gel TiO2 coating." *Solid State Phenomena* 268 (2017): 224-228. https://doi.org/10.4028/www.scientific.net/SSP.268.224

[25] Halin, Dewi Suriyani Che, Norsuria Mahmed, Mohd Arif Anuar Mohd Salleh, A. N. Mohd Sakeri and Kamrosni Abdul Razak. "Synthesis and characterization of Ag/TiO2 thin film via sol-gel method." *Solid State Phenomena* 273 (2018): 140-145. https://doi.org/10.4028/www.scientific.net/SSP.273.140

[26] Demirci, Selim, Tuncay Dikici, Metin Yurddaskal, Serdar Gultekin, Mustafa Toparli and Erdal Celik. "Synthesis and characterization of Ag doped TiO2 heterojunction films and their photocatalytic performances." *Applied Surface Science* 390 (2016): 591-601. https://doi.org/10.1016/j.apsusc.2016.08.145

[27] Tijani, Jimoh Oladejo, T. C. Totito, O. O. Fatoba, O. O. Babajide and L. F. Petrik. "Synthesis, characterization and photocatalytic activity of Ag metallic particles deposited carbon-doped TiO 2 nanocomposites supported on stainless steel mesh." *Journal of Sol-Gel Science and Technology* 83 (2017): 207-222. https://doi.org/10.1007/s10971-017-4385-0

[28] Yu, Binyu, Kar Man Leung, Qiuquan Guo, Woon Ming Lau and Jun Yang. "Synthesis of Ag–TiO2 composite nano thin film for antimicrobial application." *Nanotechnology* 22, no. 11 (2011): 115603. https://doi.org/10.1088/0957-4484/22/11/115603

[29] Hafizah, N. Z., J. M. Juoi, M. R. Zulkifli and M. A. Musa. "Effect of Silver Content on the Crystalline Phase and Microstructure of TiO2 Coating Deposited on Unglazed Ceramics Tile." *International Journal of Automotive and Mechanical Engineering* 17, no. 3 (2020): 8179-8185. https://doi.org/10.15282/ijame.17.3.2020.11.0615

[30] Mahdieh, Zahra Moridi, Shahla Shekarriz and Faramarz Afshar Taromi. "The effect of silver concentration on Ag-TiO 2 nanoparticles coated polyester/cellulose fabric by in situ and ex situ photo-reduction method—A comparative study." *Fibers and Polymers* 22 (2021): 87-96. https://doi.org/10.1007/s12221-021-9049-6

[31] Liang, Ying, ShaoHua Wang and PengFeng Guo. "Effects of Ag on the photocatalytic activity of multiple layer TiO2 films." *Materials Technology* 32, no. 1 (2017): 46-51. https://doi.org/10.1080/10667857.2015.1116821

[32] Nandiyanto, Asep Bayu Dani, Brigitta Stacia Maharani and Risti Ragaditha. "Calcium oxide nanoparticle production and its application as photocatalyst." *Journal of Advanced Research in Applied Sciences and Engineering Technology* 30, no. 3 (2023): 168-181. https://doi.org/10.37934/araset.30.3.168181